POLITECNICO DI TORINO
Repository ISTITUZIONALE

Forced response of shrouded blades with a coupled static/dynamic approach

Original
Forced response of shrouded blades with a coupled static/dynamic approach / Gulisano A.; Firrone C.M.; Zucca S.. - ELETTRONICO. - (2011). ((Intervento presentato al convegno 7th European Nonlinear Dynamics Conference tenutosi a Rome nel 24-29 July 2011.

Availability:
This version is available at: 11583/2424040 since:

Publisher:

Published
DOI:

Terms of use:
openAccess

This article is made available under terms and conditions as specified in the corresponding bibliographic description in the repository

Publisher copyright

(Article begins on next page)

03 August 2020

Forced response of shrouded blades with a coupled static/dynamic approach

Andrea Gulisano[*], Christian M. Firrone[*], Stefano Zucca[*]

[*]*Dipartimento di Meccanica, Politecnico di Torino, Torino, Italy*

Summary. A coupled static-dynamic method is proposed and applied to bladed disks with shrouds, in order to calculate the nonlinear forced response in presence of friction damping in the frequency domain. The novel approach allows to improve the already existing methods, which require a preliminary static analysis.

Introduction

Rotor blades inside turbo-machines have to resists remarkable static and dynamic forces during their operative life. To avoid high cycle fatigue (HCF) failures, it is necessary to reduce the response level increasing the damping of the system. One of the most exploited damping sources is friction damping and one of the most common configuration of friction dampers are shrouds ([1]) located at the blade tip. By means of shrouds each blade is connected to the adjacent blades and energy is dissipated by friction due to the relative displacements of the blades.

Numerical solvers are developed to compute the forced response of shrouded bladed disks in the frequency domain by means of the Harmonic Balance Method [2], studying the periodic response of the system subjected to periodic excitation as a superposition of harmonics and reducing the differential equations of motion of the system to a nonlinear, complex, algebraic system of equations. The classical approach available in the literature is based on the following steps:

1. Normal pre-loads acting on contact surfaces are calculated by means of static equilibrium equations as function of centrifugal, thermal forces acting on the system;
2. Dynamic response of the non-linear system is computed in the frequency domain with the Harmonic Balance Method using the normal pre-loads computed at step 1 as input parameters.

In this paper, a coupled static/dynamic approach, originally implemented for underplatform dampers ([3]) is implemented for the forced response calculation of shrouded bladed disks. By means of the proposed approach the step 1 of the current state-of-the-art procedure is no more necessary.

The improvement is made possible by refining the contact element [4], which represents the state of the art in the field.

Balance Equations

The balance equations of a bladed disk with shrouds are

$$M \cdot \ddot{Q}(t) + C \cdot \dot{Q}(t) + K \cdot Q(t) = F_{eo}(t) - F_C(Q,t) \,, \tag{1}$$

where M, C and K are the mass, damping and stiffness matrices, Q is the vector of nodal displacements including disk, blades and shrouds degrees of freedom, F_{eo} is a periodic excitation, whose harmonic components are called engine orders and have angular frequencies multiple of the angular speed Ω of the rotor and $F_C(Q,t)$ are the nonlinear contact forces exerted at shrouds interfaces.

In order to compute the steady-state forced response of the system, the HBM can be used and periodic displacements Q and contact forces F_C are approximated with a Fourier series

$$Q(t) = Q^{(0)} + \Re\left(\sum_{n=1}^{N} Q^{(n)} \cdot e^{in\omega t}\right) ; \quad F_C(Q,t) = F_C^{(0)} + \Re\left(\sum_{n=1}^{N} F_C^{(n)} \cdot e^{in\omega t}\right), \tag{2}$$

where ω is the rotation speed of the bladed disk and $n \cdot \omega$ is the frequency of the generic n[th] engine-order excitation. As a consequence, the differential equation (1) is turned into a set of algebraic complex equations

$$D^{(n)}(\omega) \cdot Q^{(n)} = F_{eo}^{(n)} + F_C^{(n)} \qquad \text{with } n = 0, \dots, N \,, \tag{3}$$

where $D^{(n)}(\omega) = K + in\omega C - (n\omega)^2 M$ is the nth order dynamic stiffness matrix.

In order to reduce the size of the nonlinear problem and to be able to perform calculations of real bladed disks for industrial applications, a reduced order model must be generated. The Component Mode Synthesis can be used ([5]), keeping as physical dofs the contact nodes and adding a set of slave modes large enough to model accurately the dynamics of the system.

The resulting set of reduced non-linear equations is

$$d^{(n)}(\omega) \cdot q^{(n)} = f_{eo}^{(n)} + f_C^{(n)} \qquad \text{with } n = 0, \dots, N \,, \tag{4}$$

with $Q^{(n)} = \Psi \cdot q^{(n)}$, being Ψ the reduction matrix. Inverting the dynamic stiffness matrix, the receptance notation can be finally adopted

$$q^{(n)} = r^{(n)}(\omega) \cdot \left(f_{eo}^{(n)} + f_C^{(n)}\right) \qquad \text{with } n = 0, \dots, N \,, \tag{5}$$

Since the dofs of the system can be partitioned in contact dofs q_c, where the contact forces f_c act, and non-contact dofs q_{nc}, where no contact forces are applied, the non-linear subset of balance equation is:

$$q_C^{(n)} = q_{eo,C}^{(n)} + r_{cc}^{(n)}(\omega) \cdot f_C^{(n)} \qquad \text{with } n = 0, \dots, N \quad , \tag{6}$$

being $q_{eo}^{(n)} = r^{(n)}(\omega) \cdot f_{eo}^{(n)}$ the linear response to the external excitation.

In order to avoid the inversion of the $d^{(n)}(\omega)$ matrix at each frequency ω during the force response calculation, the receptance matrix of the reduced system is computed as

$$r_{j,k}^{(n)}(\omega) = \sum_{i=1}^{N_M} \frac{\Phi_{j,k} \cdot \Phi_{k,i}}{\omega_i^2 + i \cdot 2\zeta_i \omega_i \cdot n\omega - (n\omega)^2} \quad ,$$

where ω_i, ζ_i and Φ are the natural frequency and the modal damping and the mass-normalized mode shapes of the reduced system, whose size is N_M.
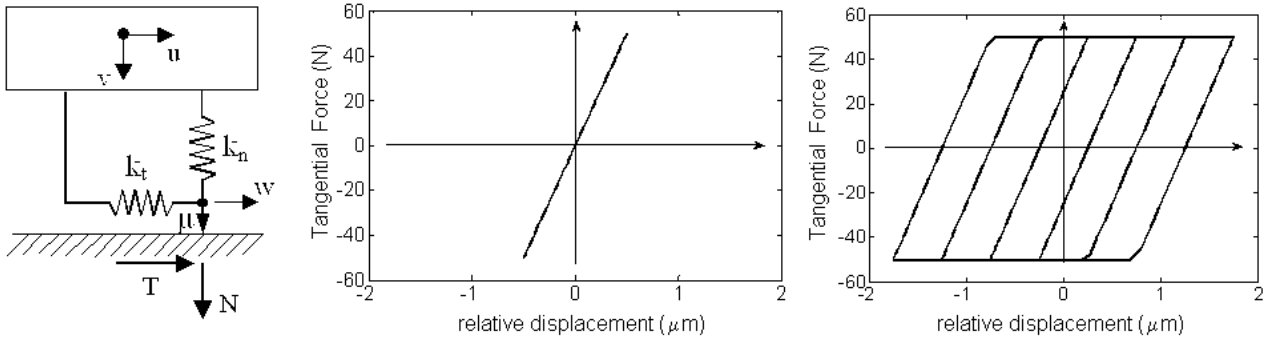
Contact Element

In order to solve the set of non-linear algebraic equations (6), it is necessary to compute the periodic contact forces at shrouds due to the relative displacement of contact points and their Fourier coefficients. The contact element used in this paper has been originally introduced in [4], but with respect to the original formulation its constitutive equations have been refined in order to couple the static and the dynamic equations of the bladed disk.

The contact element, as shown in Figure 1, is made of two springs of stiffness k_n and k_t, simulating the normal and the tangential contact stiffness and connecting the Coulomb slider to one of the body in contact. Given a periodic relative motion $u(t)$ in the tangential direction and $v(t)$ in the normal direction, defined as

$$u(t) = u^{(0)} + R\left(u^{(n)} \cdot e^{in\omega t}\right) \;\; and \;\; v(t) = v^{(0)} + \Re\left(\sum_{n=1}^{N} v^{(n)} \cdot e^{in\omega t}\right) \tag{7}$$

periodic normal and tangential contact forces can be computed. Three states are possible: *stick* when the tangential force T is lower than the Coulomb limit force μN, being μ the coefficient of friction and N the normal force, *slip* when the tangential force T reaches the Coulomb limit force μN and *lift-off* when the contact forces are null. Transitions are controlled by means of transition criteria which allow to compute numerically the transition points.

Figure 1: Contact element (left) and hysteresis cycles: full stick (middle) and stick-slip (right)

The normal contact force is modelled with the following equation

$$N(t) = max\left[k_n \cdot v_0 + k_n \cdot v^{(0)} + k_n \cdot \Re\left(\sum_{n=1}^{N} v^{(n)} \cdot e^{in\omega t}\right), 0\right] \tag{8}$$

taking into account the effect of normal relative displacement of contact point and imposing null values in case of separation of the contact points. The initial static interference, existing between the contact points before vibration starts, is defined as v_0, and the static normal force is directly linked to the value of the final static interference (or gap) $(v_0 + v^{(0)})$ of the contact points and not computed with a preliminary static analysis.

The tangential contact force depends on the contact state:

$$T(t) = \begin{cases} k_t(u(t) - w(t)) & \text{in stick conditions} \\ sgn(\dot{w}(t)) \cdot \mu \cdot N(t) & \text{in slip conditions} \\ 0 & \text{in lift-off conditions} \end{cases} \tag{9}$$

If the contact enters the slip or the lift-off state during vibration, the periodic cycle of the tangential contact force T computed by means of the constitutive equations (9) is unique. On the contrary if the vibration amplitude is not large enough to induce slip or lift-off and the contact is perfectly elastic, unique periodic tangential force T cannot be computed, since the static value $T^{(0)}$ can be included in the range

$$T_{min}^{(0)} \leq T^{(0)} \leq T_{max}^{(0)} \tag{10}$$

being $T^{(0)}{}_{min}$ the value corresponding to the elastic force tangent to the lower Coulomb limit -μN and $T^{(0)}{}_{max}$ the value corresponding to the elastic force tangent to the upper Coulomb limit +μN.

In order to have unique values of tangential contact force T(t), in case of elastic contact (full sticking conditions), the following refinement of the contact model is here proposed, based on a predictor-corrector approach.

The tangential force is initially set equal to

$$T(t) = k_t \cdot u^{(0)} + k_t \cdot \Re \left(\sum_{n=1}^{N} u^{(n)} \cdot e^{in\omega t} \right) \tag{11}$$

If

$$T_{min}^{(0)} \leq k_t \cdot u^{(0)} \leq T_{max}^{(0)} \tag{12}$$

then no correction is made. On the contrary, if during the period it is verified that

$$k_t \cdot u^{(0)} > T_{max}^{(0)} \tag{13}$$

the value of Eq. (20) is corrected as

$$T(t) = T_{max}^{(0)} + k_t \cdot \Re \left(\sum_{n=1}^{N} u^{(n)} \cdot e^{in\omega t} \right) \tag{14}$$

At the same way, if

$$k_t \cdot u^{(0)} < T_{min}^{(0)} \tag{15}$$

the value of Eq. (20) is corrected as

$$T(t) = T_{min}^{(0)} + k_t \cdot \Re \left(\sum_{n=1}^{N} u^{(n)} \cdot e^{in\omega t} \right) \tag{16}$$

By means of the proposed approach the coupled set of static and dynamic balance equations of the bladed disk with shrouded contact allows computing a unique forced response without any preliminary static calculation of simplified hypothesis about the distribution of normal pre-loads on the shroud contact area.

Once the periodic forces T(t) and N(t) are known in a local coordinate system, their Fourier coefficients can be computed, rotated in the bladed disk coordinates and added to the vector $f_C^{(n)}$ of equation (6).

Test case

In order to verify that the implemented algorithm and methods work correctly, an ad-hoc dummy blade has been designed as test case.
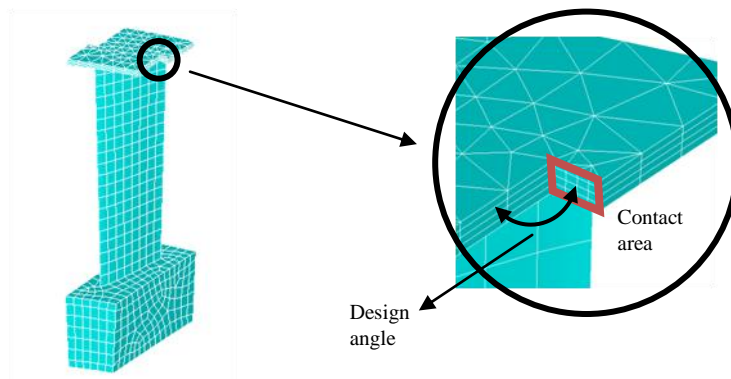

Figure 2: dummy blade used as test case and zoom of the contact area at the shroud

The contact has been distributed over 9 nodes (3x3 grid) on the contact area shown in Figure 2; the tangential and normal contact stiffness has been computed with the model developed in [7], and evenly distributed among the contact nodes.

All the blades are assumed to be identical, and so the cyclic symmetry boundary conditions ([1]) are applied to the shroud contact area, allowing to simulate the dynamics of an array of interconnected blades modelling only one of the blades, hence called the fundamental blade.

Referring to the non-linear balance equation (6), the displacements of contact nodes q_C of the fundamental blade can be divided in two sets: left contact nodes $\mathbf{q_{C,L}}$ and right contact nodes $\mathbf{q_{C,R}}$, as shown in Figure 3.
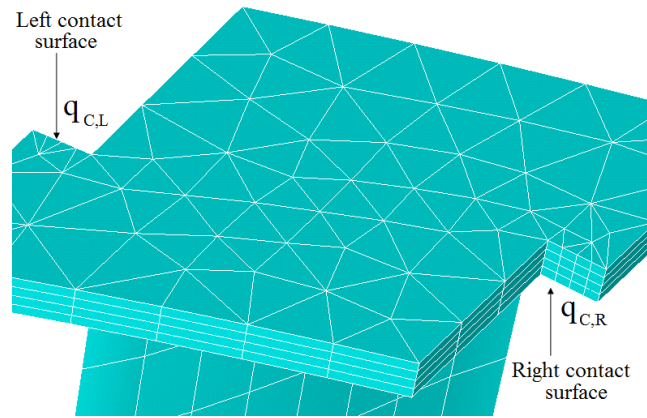
Figure 3: Cyclic symmetry: left and right contact areas of the fundamental blade.

According to the cyclic symmetry boundary conditions, the Fourier components of the relative displacements between the right contact surface of the fundamental blade and the left contact surface of the adjacent blade are expressed as

$$\Delta \boldsymbol{q_{C,R}}^{(n)} = \boldsymbol{q_{C,R}}^{(n)} - \boldsymbol{q_{C,L}}^{(n)} \cdot \boldsymbol{e^{in\varphi}} \qquad \text{with } n = 0, \dots, N \quad, \tag{17}$$

where φ is the physical inter-blade phase angle, defined as $\varphi = 2\pi/N_b$, where N_b is the number of blades.
The relative displacements defined in equation (17) are used to compute the tangential and the normal relative displacements u and v necessary to compute, with the above described contact element, the Fourier coefficients of the contact forces $\boldsymbol{f_{C,R}^{(n)}}$ acting on the right contact surface of the fundamental blade, then the contact forces acting on the left contact surface are obtained using the relationship

$$\boldsymbol{f_{C,L}^{(n)}} = -\boldsymbol{f_{C,R}^{(n)}} \cdot \boldsymbol{e^{-in\varphi}} \qquad \text{with } n = 0, \dots, N \quad, \tag{18}$$

and the vector of contact forces $\boldsymbol{f_C^{(n)}}$ of equation (6) can be assembled.

Forced response calculation

Since the contact model is able to take into account variable normal contact forces, partial lift-off may occur and, as shown in the literature, the FRF curve may exhibit the so-called jump phenomenon ([4]) and turning points on the curve as well as multiple balance conditions ω may exist in a given range of excitation frequencies. In order to compute properly the response of the system when partial lift-off occurs, a pseudo-arc length continuation method ([6]), has been adopted to solve the balance equations (6). Apart from the first frequency, when a classical Newton-Raphson method is used, The method at the kth frequency $\omega^{(k)}$ is based on a predictor-corrector approach:

1. The predictor step is performed tangent to the response curve starting from the solution at the $(k-1)^{th}$ frequency;
2. The corrector step consists in an iterative solution based on Newton-Raphson using as a search direction the direction normal to the predictor step.

At each iteration, the following steps are performed:

1. Computation of relative displacements of contact points;
2. Computation of physical displacements and forces in the time domain;
3. Harmonic components of contact forces are obtained back by means of an FFT algorithm;
4. Check of the residual of the balance equations.

The adopted procedure can be schematically represented as shown in Figure 4.
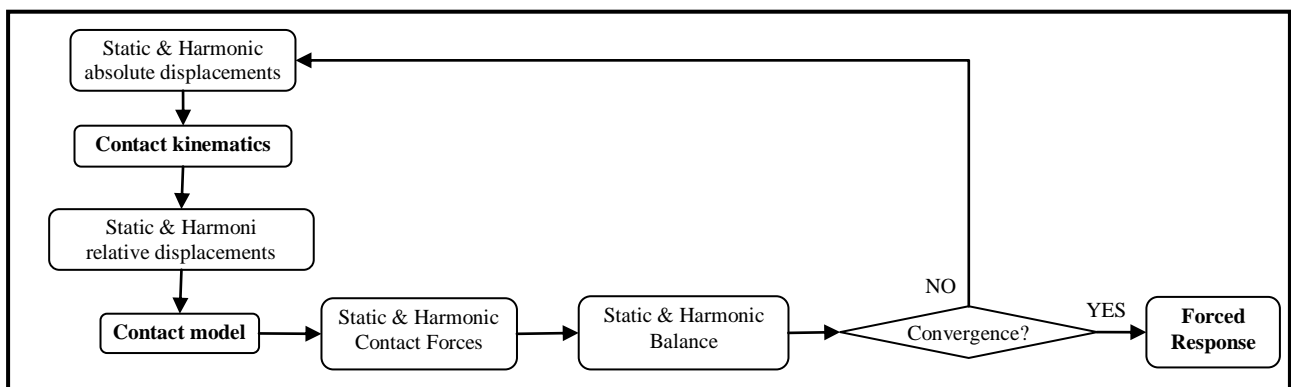

Figure 4: coupled static/dynamic balance solution algorithm

Analysis and results

The coupled method is implemented in a numerical solver to calculate the frequency response function (FRF) of the dummy bladed disk by varying the shroud design angle α and the engine order (eo) of the excitation force for different initial normal gap or interference v_0.

For the response calculation only the zero order and the fundamental harmonics have been selected.
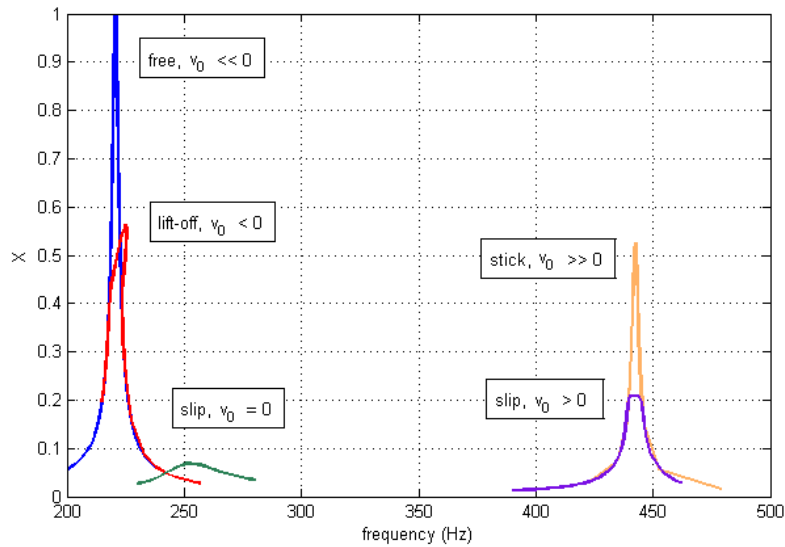
Figure 5: response curves for different initial static interference (or gap) for design angle $\alpha = 70°$.

In Figure 5 the response curves for the shroud configuration depicted in Figure 2 are shown for different values of the design static interference v_0 between adjacent blades. The typical trend of the free-slip-stick nonlinear phenomenon is clearly visible: by gradually increasing the initial interference from negative (gap) to positive values, the resonant frequency shifts to higher values than the free configuration (i.e. no contact at shroud during whole vibration cycle), and finally reaches the stick response. This behavior is due to the increase of the contact normal load at shroud contact area interfaces. In parallel, the maximum response peak shows a minimum corresponding to the maximum friction damping generated at the shroud contacts.

On the left side of the figure, a jump phenomenon is slightly visible and it produces a small hardening effect, due to partial lift-off of the contacts during vibration, as described in [4], for small negative values of the initial interference. The stable and unstable branches of that response curve have been successfully computed thanks to the pseudo-arc length continuation method.

On the contrary, on the right side of the figure there are no jump phenomena and this is a sign of the good design of the shroud contact interface adopted for this calculation.
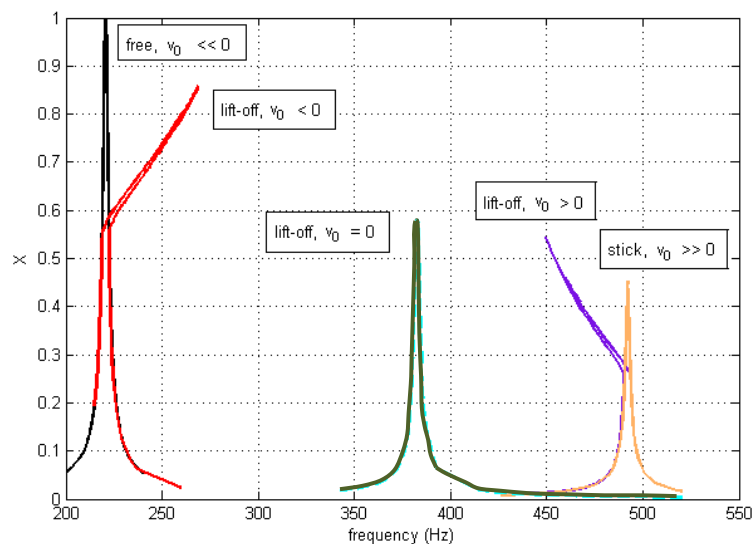
Figure 6: response curves for different initial static interference (or gap) for design angle $\alpha = 180°$.

In Figure 6 the response curves for a different shroud configuration are shown for different values of the initial interference between adjacent blades. The design angle represented in Figure 2 has been increased and the displacement components normal to the shroud contact area are now of greater significance. While in the previous ideal design case it was clearly identifiable a minimum condition between the free and full stick conditions, in this case there is a monotonous trend towards lower peak values. The minimum condition now coincides with the full stick configuration.

Given the shroud design, jump phenomena are far more evident than in the previous case, both on the free side of the figure and on the stick side. The partial lift-off on the right side of the figure causes a softening effect of the system.

In Figure 7 the response curves for different engine order excitations are shown for a constant value $v_0<0$ (i.e small gap). The shroud contact area configuration adopted is the same as the case depicted in Figure 6, where jump phenomena produced by partial lift-off during vibration cycle are more significant. Different behaviors are observed, since the value of the engine order affects the value of the inter-blade phase angle, which defines the cyclic symmetry boundary conditions applied to the fundamental blade.

First, the hardening effect (i.e. shift of the peak towards higher frequencies) increases as the engine order value grows larger, since the vibration mode of two consecutive blades tends towards the out-of-phase vibration and, as a result, the displacements normal to the contact area, which produce lift-off, become higher. Second, the vibration amplitude shows a minimum condition which is close to eo=30, showing that, for this configuration, the damping of the system reaches its maximum value in that condition.
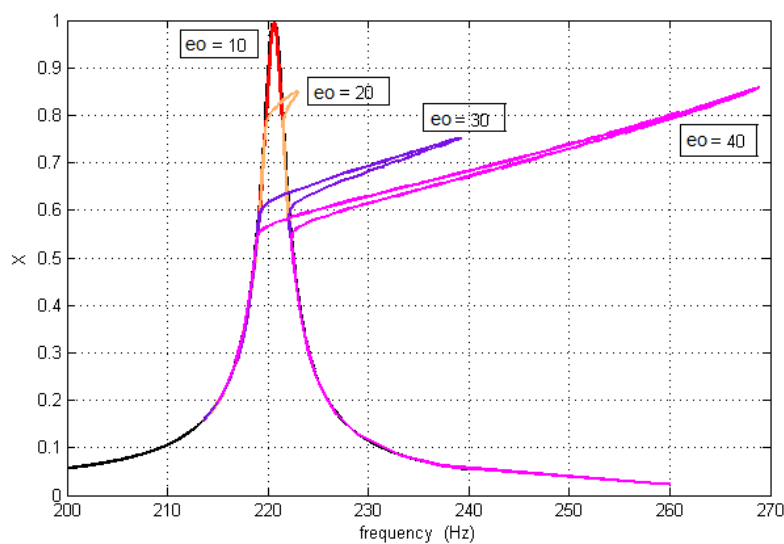

Figure 7: response curves for different engine orders of the excitation force.

Conclusions

In this paper, a coupled static/dynamic method is proposed for the forced response calculation of shrouded bladed disks. The method relies on the simultaneous calculation of the static and the dynamic balance of the system, without any preliminary static analysis. The proposed method is applied to an array of turbine blades. The forced response of the system around the first blade bending mode is computed. The validity of the proposed approach is shown and the effect of the main design parameters (i.e. initial gap/interference, shroud contact area design angle, excitation engine order) is investigated.

References

[1] Siewert C., Panning L., Wallascheck J, Richter C. (2009) Multiharmonic Forced Response Analysis of a Turbine Blading Coupled by Nonlinear Contact Forces. *Proceedings of ASME Turbo Expo 2009* GT2009-59201.

[2] Cadorna A., Coune T., Lerusse A., Geradin M. (1994) A Multiharmonic Method for Non-Linear Vibration Analysis. *Intl. J. for Numerical Methods in Engineering* VOL. 37, 1593-1608.

[3] Firrone C.M., Zucca S., Gola M.M. The effect of underplatform dampers on the forced response of bladed disks by a coupled static/dynamic harmonic balance method, *International Journal of Non-Linear Mechanics*, In press.

[4] Yang B.D., Chu M.L., Menq C.H. (1998) Stick-Slip-Separation Analysis and Non-Linear Stiffness and Damping Characterization of Friction Contacts Having Variable Normal Load. *J. Of Sound and Vibration* 210(4), 461-481.

[5] Craig R.R., Bampton M.C.C., 1968, "Coupling of Substructures for Dynamic Analyses", *AIAA Journal*, VOL. 6(7), pp.1313-1319.

[6] Chan T.F.C., Keller H.B., Arc-Length Continuation and Multi-Grid Techniques for Nonlinear Elliptic Eigenvalue Problems, *SIAM J. Sci. Stat. Comput.*, 1982, 3(2), pp. 173-194.

[7] Allara M., 2009, A model for the characterization of friction contacts in turbine blades, Journal of Sound and Vibration, vol. 320(3), pp 527-544.